Redshifting rings of power

Wayne Hu

Center for Cosmological Physics, Department of Astronomy and Astrophysics, and Enrico Fermi Institute, University of Chicago, Chicago, Illinois 60637, USA

Zoltan Haiman

Department of Astronomy, Columbia University, 550 West 120th Street, New York, New York 10027, USA

The cosmic microwave background (CMB) has provided a precise template for features in the linear power spectrum: the matter-radiation turnover, sound horizon drop, and acoustic oscillations. In a two-dimensional power spectrum in redshift and angular space, the features appear as distorted rings, and yield simultaneous, purely geometric, measures of the Hubble parameter $H(z)$ and angular diameter distance $D_A(z)$ via an absolute version of the Alcock-Paczynski test. Employing a simple Fisher matrix tool, we explore how future surveys can exploit these rings of power for dark energy studies. High-z CMB determinations of H and D_A are best complemented at moderate to low redshift ($z \lesssim 0.5$) with a population of objects that are at least as abundant as clusters of galaxies. We find that a sample similar to that of the ongoing SDSS luminous red galaxy survey can achieve statistical errors at the $\sim 5\%$ level for $D_A(z)$ and $H(z)$ in several redshift bins. This, in turn, implies errors of $\sigma(w) = 0.03$–0.05 for a constant dark energy equation of state in a flat universe. Deep galaxy cluster surveys such as the planned South Pole Telescope survey can extend this test out to $z \sim 1$ or as far as redshift follow-up is available. We find that the expected constraints are at the $\sigma(w) = 0.04$–0.08 level, comparable to those of galaxies and complementary in redshift coverage.

I. INTRODUCTION

Cosmic microwave background (CMB) measurements have now established the sound horizon and horizon at matter-radiation equality as standard rulers for cosmology. Current errors on the absolute scales are approximately 2% and 8%, respectively [1], and will continue to improve as higher angular resolution data further resolve the morphology of the acoustic peaks. From the angular scale subtended by these rulers, the CMB provides a comparably precise measurement of the angular diameter distance D_A to the epoch of recombination.

These rulers appear in the matter power spectrum as a smooth turnover at the matter-radiation horizon, a sharper drop at the sound horizon, and a series of acoustic oscillations at harmonics of the sound horizon [2,3]. The acoustic features are close analogues of the CMB peaks and cause variations of order 10% in power. They are preserved out to nearly the nonlinear scale at any given redshift [4]. The whole set of features does not evolve with redshift in the linear regime in the absence of a significant massive neutrino component to the dark matter. Matching of the observed features with the template provided by the CMB provides cosmological distance measures $D_A(z)$ based on the same physics and method as the CMB [5,6]. There is, in fact, more information in a three-dimensional redshift survey since the redshift dimension measures the evolution of the Hubble parameter $H(z)$ and so the dark energy density evolution directly [7].

These features appear as *rings* in the two-dimensional angular and redshift space. At $z = 0$, the angular diameter distance D_A and the Hubble parameter H depend only on the current expansion rate. Here the rings are circular and the

measurement of their location returns the Hubble constant H_0 [5]. In the range $0 < z \lesssim 1$, the scalings of D_A and H depend on the dark energy evolution, whereas for $z \gtrsim 1$ they are expected to return to the matter-dominated scalings provided by the CMB. The relative distortion between the redshift and angular dimensions provides the Alcock-Paczynski [8] test for dark energy. Here, we show that the absolute distortion can be measured from the absolute calibration of the standard rulers.

Recently there have been several studies of the utility of acoustic features to constrain cosmology at $z = 1$–3 emphasizing the extended range of the linear regime and the large volumes encompassed by surveys with moderate angular dimensions (e.g., a few hundred square degrees) [7,9,10]. High-z surveys would provide important consistency checks with the high-z CMB as well as limit any residual dark energy component at those epochs. However, given the CMB determination, the most important regime to probe is at moderate to low redshift, since this provides the largest lever arm in distance.

The quantitative tools developed to address these issues have focused on the angle-averaged $P(k)$ which entangles and degrades information on D_A and H [9]. In contrast, the separately developed general tools for analyzing the information in redshift surveys at cosmological distances are complete but computationally costly to implement [11]. This difficulty has prevented a full exploration of the use of two-dimensional power spectrum rings given a CMB power spectrum template and the requirements that their measurement places on surveys. Here we generalize the approximate mode counting estimates for power spectrum measurement errors [12] to the two-dimensional space and quantify the information through a Fisher matrix approach.

We begin in Sec. II with a discussion of the cosmological distortion of power spectrum rings. We continue in Sec. III with the mode counting technique for estimating the capabilities of redshift surveys. In Sec. IV, we describe two mock surveys for illustration purposes, one based on the ongoing Sloan Digital Sky Survey (SDSS) luminous red galaxy (LRG) survey at intermediate redshifts and the other based on a deep galaxy cluster survey such as the planned South Pole Telescope (SPT) survey [13]. We examine potential cosmological constraints on distances, the Hubble parameter, and the dark energy in Sec. V. Their dependence on survey and other assumptions is explored in in Sec. VI. We discuss the results in Sec. VII.

Throughout this paper, we take as the fiducial cosmology a flat CDM with a cosmological constant (ΛCDM) model with baryon density $\Omega_b h^2 = 0.024$, matter density $\Omega_m h^2 = 0.14$, scalar slope $n_s = 1$, dark energy density in units of the critical density $\Omega_{DE} = 0.72$ (or Hubble constant $H_0 = 100h$ km s^{-1} Mpc^{-1} with $h = 0.72$), initial curvature $\delta_\zeta = 5.07 \times 10^{-5}$ at $k = 0.05$ Mpc^{-1} (or present normalization $\sigma_8 = 0.9$ and reionization optical depth $\tau = 0.17$), and a constant dark energy equation of state $w = p_{DE}/\rho_{DE} = -1$. These values are consistent with recent determinations from Wilkinson Microwave Anisotropy Probe (WMAP) [1].

II. RINGS OF POWER

Geometrical distortions at cosmological distances are described by the Friedmann-Robertson-Walker spatial line element

$$ds^2 = a^2(dD^2 + D_A^2 d\Omega). \qquad (1)$$

The metric elements are related to the observable redshift as $a = (1+z)^{-1}$ for the scale factor, $dD = dz/H$ for the radial distance D, and $D_A = R \sin(D/R)$ for the angular diameter distance, where the radius of curvature $R = H_0^{-1}\sqrt{\Omega_{tot}-1}$, and Ω_{tot} is the total density in units of the critical density. All distances are in comoving coordinates. The Hubble parameter is given by the Friedmann equation as

$$H^2(z) = \frac{8\pi G}{3}\rho_{tot}(z) - \frac{1}{(aR)^2}, \qquad (2)$$

with $H_0 = H(z=0)$. Since the conversion from the observable angular and redshift space coordinates to physical coordinates depends on the metric, a "standard ruler" of a known physical size can be used to measure cosmology.

Suppose now that we have a survey of some biased tracer of the mass, effectively at some redshift z_s. The two-point correlation or power spectrum of the objects acts as the standard ruler. Since power spectrum modes are usually quoted in units of inverse length scale, let us choose the fiducial cosmology for the conversion

$$k_\perp^{fid} = \frac{\ell}{D_A^{fid}(z_s)},$$

$$k_\parallel^{fid} = \frac{2\pi}{\lambda_z}\frac{\Delta z}{\Delta D} \approx \frac{2\pi}{\lambda_z}\frac{dz}{dD}$$

$$= \frac{2\pi}{\lambda_z}H^{fid}(z_s), \qquad (3)$$

where λ_z is the radial wavelength in redshift and ℓ is the angular wave number or multipole. Note that in our fiducial flat cosmology $D_A = D$. The true modes being probed by a given ℓ and λ_z are

$$k_\perp = s_\perp k_\perp^{fid},$$

$$k_\parallel = s_\parallel k_\parallel^{fid}, \qquad (4)$$

where the shift parameters are

$$s_\perp = \frac{D_A^{fid}}{D_A},$$

$$s_\parallel = \frac{\Delta D^{fid}}{\Delta D} \approx \frac{H}{H^{fid}}. \qquad (5)$$

In the linear regime, the power spectrum of the tracer objects reflect the underlying mass power spectrum $P(k)$ modified by redshift space distortions as [14]

$$P_s(k_\perp, k_\parallel) = \left[1 + \beta\left(\frac{k_\parallel}{k}\right)^2\right]^2 b^2 P(k),$$

$$k^2 = k_\perp^2 + k_\parallel^2, \qquad (6)$$

where b is the linear bias assumed to be scale independent (e.g., [15]). Deep in the linear regime, the distortion parameter

$$\beta = \frac{1}{b}\frac{d\ln D_{grow}}{d\ln a}, \qquad (7)$$

where D_{grow} is the linear growth rate; we alternatively consider β to be a free parameter to reflect uncertainties in the distortion approaching the nonlinear regime. With prior knowledge of the underlying form of $P(k)$ from the CMB, the shifting in the observational domain measures the angular diameter distance D_A and Hubble parameter H through Eq. (5).

The redshift power spectrum is shown for the fiducial model in Fig. 1. Note that the locations of the rings remain undistorted in the presence of the smooth linear redshift space distortion but not under a change in the cosmology. Note further that the usual Alcock-Paczynski test utilizes only the departure of the rings from perfect circles [8], regardless of their radius. We utilize more information here: the absolute distortion, including the radius. Hence D_A and H can in principle be measured independently. Moreover, in the
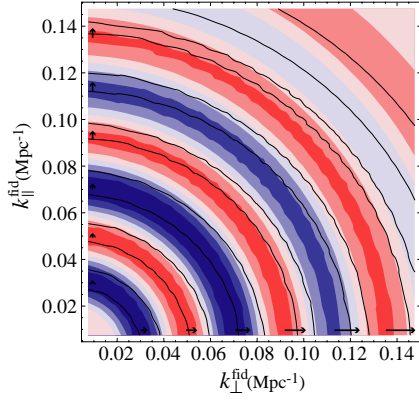
FIG. 1. Acoustic rings in the two-dimensional power spectrum $P_s/\bar{P}_s - 1$ with a smooth component $\bar{P}_s$ [3] removed to highlight the features; shaded contours are spaced by 0.02. The locations of the features are preserved in the presence of linear redshift space distortions here at $z = 0.45$ and $b = 3.5$. Cosmology distorts the rings here shown with $w = -2/3$, $\Omega_{DE} = 0.62$, and $h = 0.61$, which preserves the CMB-determined high-z D_A and H. Arrows indicate the shifting of extrema; solid curves trace the extrema for $w = -2/3$, to be compared with the shaded contours of the fiducial $w = -1$ cosmology. Jaggedness reflects our k-cell discretization.

complete absence of template information from the CMB, cosmological constraints on the dark energy become substantially weaker and subject to uncertainties in the correction of redshift space distortions [11].

III. ERROR ESTIMATES

To estimate potential constraints on cosmology from the rings, we begin by considering statistical errors on the measured two-dimensional power spectrum. Statistical errors arise from the finite number of spatial samples of the clustering and that of the tracer objects contributing shot noise. These will depend on the effective volume probed by the sample, which we will parametrize by the solid angle A_s, redshift z_s, and redshift extent Δz_s of the survey.

The survey dimensions define a set of fundamental modes or equivalently a fundamental unit in three-dimensional k space. Each of these units can be considered an independent measurement of the power spectrum and so the net error on a larger cell in k space over which the power spectrum is measured is simply $(2/N)^{1/2}$, where N is the number of fundamental units in the cell (see, e.g., [16]). The shot noise from the finite number density of the tracers increases the fractional errors by $(1 + 1/\bar{n}P_s)$ to give a net error of [12]

$$\left(\frac{\Delta P_s}{P_s} \right)^2 = \frac{2}{V_k V_{\text{eff}}}, \tag{8}$$

where

$$V_{\text{eff}}(k) = \int dV_s \left[\frac{\bar{n}(z_s) P_s(k)}{1 + \bar{n}(z_s) P_s(k)} \right]^2 \tag{9}$$

is the effective volume probed and

$$V_k = \frac{2 \pi \Delta(k_\perp^2) \Delta k_\parallel}{(2\pi)^3} \tag{10}$$

is the k-space volume of the double ring of positive and negative $k_\parallel$. For a roughly constant number density, the variance scales as $1/V_s$ or $1/A_s$. The covariance between cells is negligible so long as $\Delta k_\perp \gg (D_A^{\text{fid}} A_s^{1/2})^{-1}$, $\Delta k_\parallel \gg (\Delta z_s / H^{\text{fid}})^{-1}$ [16].

Power spectra error estimates can be converted into error estimates on cosmological parameters. Given a set of parameters p_μ, the Fisher matrix

$$F_{\mu\nu} = \sum_i \frac{\partial \ln k_\perp^2 k_\parallel P_{si}}{\partial p_\mu} \frac{V_{ki} V_{\text{eff } i}}{2} \frac{\partial \ln k_\perp^2 k_\parallel P_{si}}{\partial p_\nu} \tag{11}$$

approximates the variance of the parameter estimates as $\sigma^2(p_\mu) = (\mathbf{F}^{-1})_{\mu\mu}$. Note that fractional errors on $k_\perp^2 k_\parallel P(k)$ are the same as for $P(k)$ for sufficiently small cells and so this prescription follows from simple error propagation.

The subtlety in Eq. (11) lies in the choice of the observable $k_\perp^2 k_\parallel P_{si}$. Here i indexes an array of cells in two dimensions that are evaluated with fixed observable $k_\perp^{\text{fid}}, k_\parallel^{\text{fid}}$ and hence $k_\perp$ and $k_\parallel$ that shift with the cosmological parameters p_μ. This prescription is the high-z analogue of bands in h Mpc^{-1}. Likewise, the weighting $k_\perp^2 k_\parallel \propto s_\perp^2 s_\parallel$ reflects the observable angular and redshift space variance and is the high-z analogue of quoting power spectra in units of h^{-3} Mpc^3. Thus some sensitivity to the shifts is coming from the change in the volume element with cosmology. This information is degenerate with an amplitude change in the power spectrum at the given redshift.

IV. MOCK SURVEYS

Tracer objects must have a sufficient number density and clustering strength for a measurement of the power spectrum in the presence of shot and other noise sources. If systematic errors can be controlled, integration time is best spent in tracing a large volume with the lowest-abundance objects that suffice. The power spectrum error estimates of the previous section provide a simple criterion for the choice of astrophysical tracers such as galaxies and galaxy clusters.

For definiteness we will mock up the tracer objects as dark matter halos to a limiting mass in the theoretical mass function [[17], Eq. (B3)] that approximately matches the number densities expected from a given observation. This prescription also fixes the bias through the halo prescription [18] as modified by [19] for the improved mass function. Note that the larger bias of the high-mass objects partially offsets their lower number density. Shown in Fig. 2 is the halo mass scale at which the signal to noise ratio $\bar{n}P_s(k_\perp = k, k_\parallel = 0) = 2$ for the fiducial cosmology for k values corresponding to the extrema of the acoustic oscillations [9]. For intermediate redshifts, objects with the number density and bias of low-mass clusters and groups suffice.

Let us therefore consider two mock surveys, one based on galaxies and the other on clusters. We choose parameters that are roughly similar to the SDSS main and LRG samples [20]
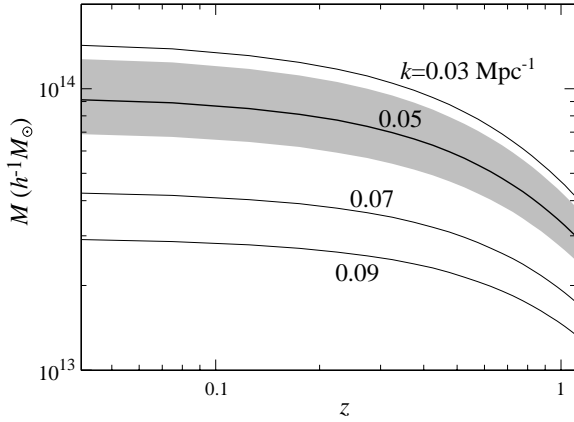
FIG. 2. Tracers of power at the peak wavelengths of the acoustic rings with a signal to shot noise $\bar{n}P_s=2$ (range of 1.5–2.5 shaded for the $k=0.05$ ring). Tracers are quoted in terms of the parent halo mass threshold which parametrizes the number abundance and bias of the tracer population.

and a deep cluster survey such as the planned SPT survey [13]. Specifically, we take the number density of LRGs to be $\bar{n}=1\times10^{-4}h^3$ Mpc^{-3} at $z=0.3$ [20] and so mock the population with halos of $M>10^{13.5}h^{-1}M_\odot$ and hence an average bias $b\approx2$. We divide the sample into three bins of $\Delta z=0.1$ from $z=0.1$ to 0.4. We take the main survey to consist of galaxies with $\bar{n}=3\times10^{-3}h^3$ Mpc^{-3} corresponding to a population with $M>10^{12.1}h^{-1}M_\odot$ and $b\approx1$ in a single volume from $z=0$ to 0.1. We take both samples to cover a sky area of $A_s=10000$ deg^2. Note that the LRG population is well placed for measuring the acoustic rings in terms of both number density and redshift.

We take the cluster survey to cover $A_s=4000$ deg^2, to have a constant mass threshold of $M>10^{14.2}h^{-1}M_\odot$ [21], and to extend in the range $0.1<z<1.3$ binned in steps of $\Delta z=0.2$. We will assume that the cluster survey has follow-up redshifts on all clusters ($N\approx25000$). We explore the precision required in the redshifts and degradation suffered from lack of high-z follow-up ($N\approx14000$; $0.1<z<0.7$) in Sec. VI. For both mock surveys we approximate the number densities to be constant across the redshift bin evaluated at the angular diameter distance midpoint.

To be conservative, we marginalize the bias and hence the information contained in the growth of structure. This procedure isolates the geometric aspect of the test so that a misestimate in the tracer bias simply scales the signal to noise ratio and does not bias the results. We leave a full consideration of the cosmological information in the power spectrum to a separate work [22] (see also [23]).

We take 29^2 linearly spaced k cells from $k_{\perp,\parallel}=0.005$ to 0.15 Mpc^{-1} defining a cylinder in three-dimensional k space. Note that the total k volume we utilize is a factor of 1.5 larger than the volume of a corresponding sphere with a radius $k_{\max}=k_{\perp,\max}=k_{\parallel,\max}$; a cylindrical volume facilitates tests of the required redshift resolution (see Sec. VI). The maximum k in each direction hits the nonlinear scale at $z=0$ and the measurements will be somewhat degraded by nonlinear corrections to the redshift space distortion and the

washing out of features in the mass power spectrum [4]; we explore the dependence of the results on $k_{\max}$ in Sec. VI below.

We account for uncertainties in the CMB template matter power spectrum by allowing $(\Omega_bh^2,\Omega_mh^2,n_s)$ to vary from the fiducial model. Current CMB uncertainties are at the level $\sigma(\ln\Omega_bh^2)=0.04$, $\sigma(\ln\Omega_mh^2)=0.08$, $\sigma(n_s)=0.03$ [1]. We take $(0.01,0.01,0.01)$ as a projection of future CMB constraints implemented by the addition of $(F_{\text{prior}})_{\mu\nu}=\delta_{\mu\nu}\sigma(p_\mu)^{-2}$ to the Fisher matrix of Eq. (11). We discuss the effect of weakening these priors in Sec. VI.

For reference, the Planck satellite can in principle achieve errors of $(0.009,0.0065,0.004)$ [25]. Moreover, the combination of WMAP with high-resolution ground and balloon based measurements should also be able to reach this level eventually. When implementing Planck-specific priors in the consideration of dark energy constraints, we employ the full Fisher matrix forecast rather than the diagonal approximation.

Aside from these three parameters, we also include uncertainties due to the initial normalization $\ln\delta_\zeta$, the reionization optical depth τ, and the tensor-scalar ratio T/S, when considering prior knowledge from the CMB. The remaining parameters in the Fisher matrix are then $\ln\beta$, $\ln b$, and the dark energy parameters. We take weak priors $\sigma(\ln\beta)=\sigma(\ln b)=0.4$ unless otherwise stated.

V. COSMOLOGICAL CONSTRAINTS

A cosmology parametrized by a discrete set of shift parameters $s_\parallel(z_s)$ and $s_\perp(z_s)$ away from a fiducial cosmology returns the distance and Hubble parameter as $D_A=D_A^{\text{fid}}/s_\perp$ and $H=H^{\text{fid}}s_\parallel$ at the given redshift. This parametrization is valid for any model of dark energy evolution, including those involving spatial curvature $R\neq0$, and is a complete description for geometrical tests. The underlying assumption is that the dark energy remains smooth on survey scales and hence does not affect the shape of the power spectrum.

The projected constraints on the shift parameters for the galaxy and cluster mock surveys are shown in Fig. 3. To eliminate the information coming from redshift space distortions and the growth of structure, we marginalize β and the bias b with weak priors.

To understand the efficacy of the projected constraints for dark energy studies, recall that the fiducial cosmology is chosen so that $D_A^{\text{fid}}(z_*)$ and $H^{\text{fid}}(z_*)$ hit the central value of the WMAP results [1]. Thus $s_\parallel,s_\perp$ are constrained to lie near unity at z_*, the recombination redshift. In terms of cosmological parameters, a fixed $H^{\text{fid}}(z_*)$ implies a fixed Ω_mh^2.

Deviations due to the influence of the dark energy mainly appear at low redshift. In a simple constant-w parametrization of the dark energy, the high-redshift constraint requires Ω_{DE} to decrease as w increases since

$$\rho_{\text{DE}}(z)=\frac{3H_0^2}{8\pi G}\Omega_{\text{DE}}(1+z)^{3(1+w)}. \qquad (12)$$

In Fig. 3, we show an example satisfying this constraint with $w=-2/3$ and hence $\Omega_{\text{DE}}=0.62$. This constraint tends to
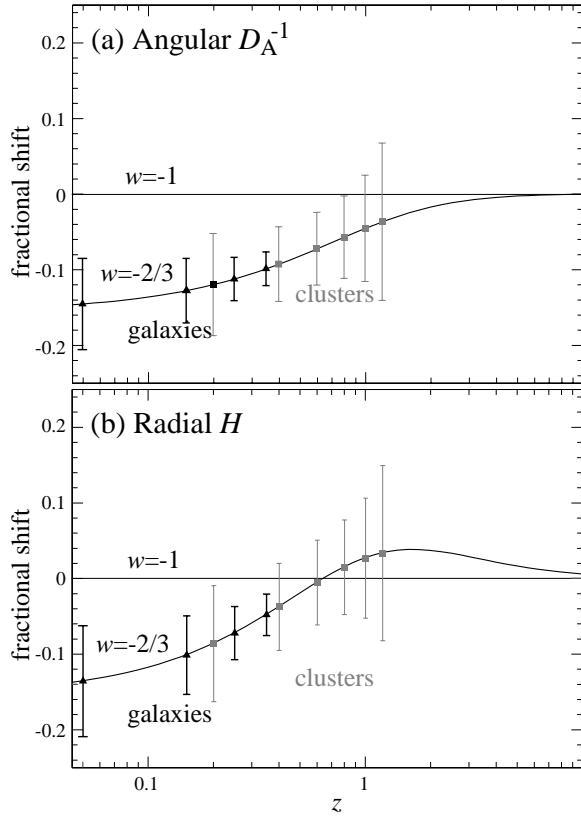
FIG. 3. Projected constraints on the fractional shifts ($s_{\perp,\parallel} - 1$) in (a) D_A and (b) H from the fiducial model given the galaxy and cluster surveys specified in Sec. IV. Constraints are marginalized over the redshift space distortion β and the bias parameter in each bin separately. The high-z tails of the D_A and H curves are constrained by the CMB, currently to a precision of $\sim 2\%$ and $\sim 4\%$ [$\sigma(\ln \Omega_m h^2) = 0.08$]; projections assume a future improvement to $\sigma(\ln \Omega_m h^2) = \sigma(\ln \Omega_b h^2) = \sigma(n_s) = 0.01$ for the power spectrum template, but the difference is not substantial.

make dark energy effects disappear more rapidly as z is increased than variations, say, at a fixed Ω_{DE}. Note that at some redshifts the shift in the parallel and perpendicular directions have the opposite sign. An angle averaging of the power spectrum [9] would recover an average shift of

$$\bar{s} \approx \frac{2}{3} s_\perp + \frac{1}{3} s_\parallel, \qquad (13)$$

and hence this procedure both degrades the signal and complicates the interpretation for a model of the dark energy with arbitrary evolution.

Since $s_\parallel(z=0)$ and $s_\perp(z=0)$ both return H_0/H_0^{fid}, the low-redshift side directly measures the Hubble constant. In fact, the best single redshift at which to complement the CMB is $z=0$ because a change in Ω_{DE} implies a change in h in a flat universe, since $\Omega_m h^2 = (1 - \Omega_{DE}) h^2$ is fixed by the high-z Hubble parameter determination. Note the large deviation between the curves in Fig. 3 at $z=0$, reflecting an $h = 0.61$ and rapid return to the fiducial values for $z \gtrsim 1$.

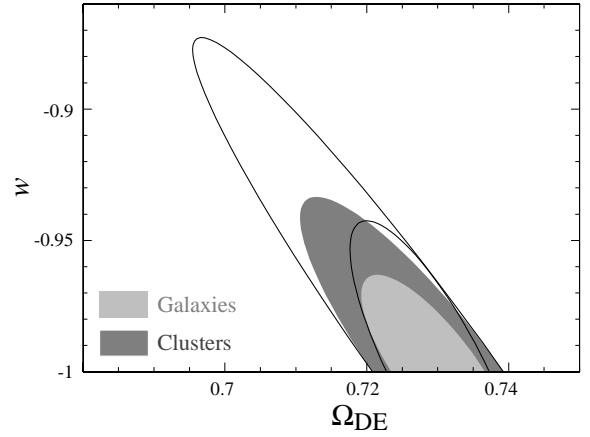The galaxy sample therefore provides the best complement to the high-z CMB constraint for both D_A and H, or

FIG. 4. Projected 68% C.L. constraints on w, Ω_Λ from the galaxy and cluster surveys described in Sec. IV in combination with Planck priors on the $P(k)$ template and $D_A(z_*), H(z_*)$. Filled ellipses represent constraints with a global bias amplitude marginalized and with β given by linear theory; open ellipses marginalize a scaling factor to β and also the bias separately at each redshift.

equivalently w. It can yield a highly significant separation between the $w = -2/3$ and $w = -1$ fiducial models and potentially even an internal detection of the evolution in D_A^{-1} and H due to the dark energy. Even though the clusters do not have the number density to be optimal for this test, their ability to probe intermediate redshifts would be invaluable for constraints on dark energy evolution.

Joint constraints on the dark energy equation of state w depend on how well the CMB fixes the high-z tail of the curves in Fig. 3. In Fig. 4 we employ a projection of Planck capabilities from [25] and combine them with the constraints from the mock galaxy and cluster surveys redshift slices by adding the Fisher matrices. Here we assume a dark energy parametrization given by (w, Ω_{DE}) in a flat universe. The filled ellipses represent constraints with a single overall bias parameter b marginalized and with β given by the linear theory prediction. We discuss the sensitivity to these assumptions in Sec. VI. Note that the geometric constraint from the CMB peaks alone follows a pure $D_A(z_*)$ degeneracy curve in the (Ω_{DE}, w) plane, and so the ability to measure Ω_{DE} and w comes from the rotation of the degeneracy curves provided by measurements of D_A and H at lower redshifts.

For the galaxy survey, the net constraint on a constant w is $\sigma(w) = 0.024$ and $\sigma(\Omega_{DE}) = 0.007$. For the cluster survey, the net constraint is still a comparable $\sigma(w) = 0.04$ and $\sigma(\Omega_{DE}) = 0.013$ because of the higher bias and extended $\Delta z = 1.2$ assumed. At the high-z end, constraints become degenerate with those of the CMB itself for models close to the fiducial model. Again, it is important to bear in mind that tracking the return to the CMB values in D_A and H would be important for any future detection of a dynamical dark energy component. This is especially true for models with a redshift-dependent equation of state $w(z)$ where the dark energy can contribute to the energy density even at high z.

VI. EXPLORING ASSUMPTIONS

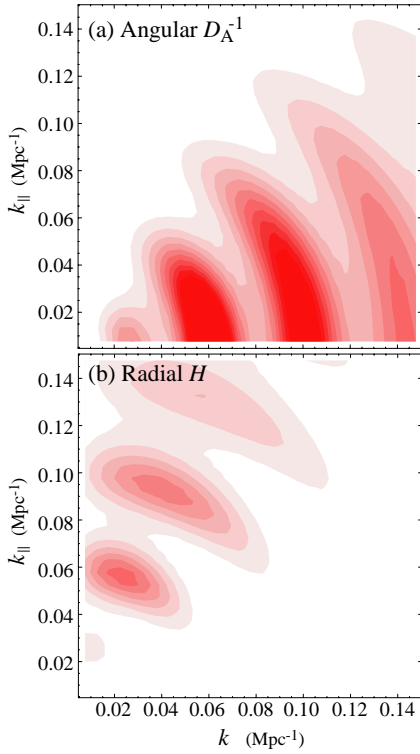The Fisher approach enables us to explore efficiently the physical origin of the cosmological information and the de-

FIG. 5. Contributions to the Fisher matrix showing the localization of information on D_A (or $s_\perp$) and H (or $s_\parallel$) in the $(k_\perp, k_\parallel)$ plane. Here $z = 0.4$, and we have taken clusters with a mass threshold of $10^{14.2} h^{-1} M_\odot$ ($\bar{n} = 8 \times 10^{-6} h^3$ Mpc^{-3}, $b = 3.4$). Notice the concentration of information at the rise and fall of the acoustic rings, the drop in information at high k due to shot noise, and the k-space volume weighting of the sample variance, which pulls the $s_\parallel$ information away from the vertical axis.

pendence of the projected constraints on our assumptions. The main assumptions are the detectability of the acoustic rings, the extent of the linear regime, the determination of redshifts for the objects, the number density of tracers, and the prior constraints.

It is instructive to consider first the source of the cosmological information. In Fig. 5 we show the contribution to the Fisher matrix for the parameters $s_\parallel$ and $s_\perp$. Here we take the mock cluster survey at $z = 0.4$. For illustrative purposes, we have first subtracted out the constant factor in the derivatives provided by the volume weighting $k_\perp^2 k_\parallel \propto s_\perp^2 s_\parallel$ as this is degenerate with the normalization [see the discussion following Eq. (11)]. Note that any constant factor is degenerate with normalization and so it is only the variations that carry independent information.

Not surprisingly, $s_\perp$ (or D_A) gains most of its information from modes nearly perpendicular to the line of sight and with $k \lesssim 0.1$ due to the shot noise at high k; nonlinearity also limits the information content on a comparable scale. The influence of the acoustic rings is clearly visible, with the largest effect being between the extrema. However, even the information in $s_\parallel$ is weighted toward nonzero $k_\perp$ due to increase in sample variance from the small k space around $k_\perp = 0$. Furthermore, estimates of $s_\perp$ and $s_\parallel$ come from nearly nonover-

lapping k cells and hence yield nearly independent determinations of D_A and H.

A quantification of the amount of information coming from the acoustic rings versus the broader features at the matter-radiation and sound horizons is important for the planning of surveys. The recovery of sharp features places stringent requirements on the survey geometry and argues for a large contiguous survey region. To address this question we replace the numerically calculated $P(k)$ from an Einstein-Boltzmann code with a smooth fit which retains both the matter-radiation bend and sound horizon drop but not the oscillations [3]. Constraints on H and D_A then degrade by a factor of 1.7 for the LRG galaxies.

The acoustic rings become even more important if the $P(k)$ template is not well determined by the CMB. Weakening the prior constraints on the template parameters $(\Omega_b h^2, \Omega_m h^2, n_s)$ to the current level (which may also be viewed as a rough proxy for future uncertainties due to massive neutrinos, scale-dependent bias, and running of the tilt [22,24]) causes a degradation by a factor of ~ 1.1 for the LRG galaxies in the presence of the acoustic rings but a factor of 2.2 in their absence. The acoustic rings therefore help make this geometric test robust to uncertainties in the power spectrum template.

The extent to which the information in the acoustic rings can be recovered with broad windows from a noncontiguous region of sky is beyond the scope of the mode counting approximation used here. It is best addressed with the full pixel, or more generally mode, correlation matrix formalism [11]. Here we simply note that, with prior knowledge of the power spectrum template from the CMB, accurate knowledge of the power spectrum window functions for the modes induced by the survey geometry may in some circumstances suffice for the measurement of D_A and H.

Because much of the information is coming from the acoustic rings, the most critical prior assumption we have made is the extent of the linear regime. Changing k_{max} from 0.15 to 0.075 Mpc^{-1} degrades the distance and Hubble errors for the LRG galaxies by a factor of ~ 2. These degradation factors are less pronounced for clusters where the higher rings are lost in the shot noise (see Fig. 5). Furthermore, at higher z the nonlinear scale k_{nl} moves out to higher k; a more detailed treatment would take $k_{max} \propto k_{nl}(z)$ [9]. Translated into constraints on w, moving $k_{max} = 0.15$ Mpc^{-1} to 0.075 Mpc^{-1} takes $\sigma(w)$ from 0.024 to 0.051 for the galaxy survey and 0.04 to 0.06 for the cluster survey.

The redshift resolution required by the cluster survey is also less stringent than for the galaxy survey. Examination of Fig. 5 shows that most of the information on both D_A and H comes from modes with $k_\parallel < 0.06$ Mpc^{-1} ($\lambda_z = 0.03$ at $z = 0.4$). For the cluster survey, excluding higher $k_\parallel$ degrades D_A by 1.2 and H by 1.7 for the $z = 0.3 - 0.5$ band and less for the higher redshift bands. With an improvement in photometric redshift techniques and averaging over cluster members, costly spectroscopic follow-up could potentially be avoided.

The mass threshold and follow-up redshift range of the cluster survey also affect potential constraints. The rarity of high-z clusters due to the steepness of the mass function

makes a low-mass threshold crucial for the recovery of information at $z \sim 1$. The requirement is less stringent for measuring a constant w since the lower redshift clusters suffice in the determination. With $M > 10^{14} h^{-1} M_\odot$, $\sigma(w)$ improves by 1.5; with $z < 0.7$ it degrades by 1.3. Increasing the sky coverage of the survey decreases the errors as $A_s^{-1/2}$ to the ultimate limit of an improvement by a factor of 3 for full-sky coverage in the cluster survey.

Removing the weak prior on β [$\sigma(\ln \beta) = 0.4$] has a negligible effect on galaxies constraints and causes a factor of ~ 1.2 degradation for the cluster D_A and H constraints. The weak prior on the overall bias [$\sigma(\ln b) = 0.4$] also has little effect on the constraints. An improvement in prior knowledge to the percent level would substantially assist constraints due in part to the degeneracy between the power spectrum normalization and the volume effects in the shift [see the discussion following Eq. (11)]. Likewise, a further weakening of the prior knowledge to account for bias evolution uncertainties by considering the bias at each redshift slice as an independent parameter degrades projections for $\sigma(w)$ by a factor of 1.6 for the galaxies and 1.9 for the clusters as shown in Fig. 4 (open ellipses).

VII. DISCUSSION

The cosmic microwave background provides a template for power spectrum features in the linear regime, or equivalently a set of absolutely calibrated standard rulers for cosmology. We have provided simple tools to estimate the cosmological information contained therein. Angular diameter distances and the Hubble parameter can be measured in a purely geometric way that involves only the well-understood physics of the CMB and linear perturbation theory. A detection of the acoustic rings would assist in making the angular diameter distance measurement robust, but is not strictly required if one assumes continued improvement in the determination of the power spectrum template from the CMB. Conversely, current determinations of the power spectrum template suffice if the acoustic rings are detected.

The tools we have introduced should assist in planning future surveys to complement current cosmological knowl-

edge. When actually analyzing data, of course they must be replaced by more sophisticated tools that account for cosmological evolution across the survey subvolumes, the angular mask, the radial selection, and the curvature of the sky [11]. The extent of the linear regime and nonlinear corrections in the translinear regime must also be addressed more carefully in simulations [4].

These estimates show that power spectrum rings at intermediate redshifts $z < 1$ hold great promise for cosmology. The angular distortion can be measured with objects that are at least as abundant as clusters of galaxies. At $z < 0.4$ the ongoing SDSS LRG survey can precisely determine the Hubble constant, the best complement to the CMB, and potentially measure the dark energy driven evolution of D_A and H separately to obtain net constraints at the $\sigma(w) = 0.03–0.05$ level, depending on the extent of the linear regime. At intermediate redshifts, clusters can probe the onset of dark energy domination with comparable precision $\sigma(w) = 0.04–0.08$, ranging from perfect constraints on bias evolution to no constraints. Cluster distance and even crude Hubble parameter measurements do not require high resolution in redshift and are potentially possible with photometric redshifts if the errors can be reduced to $\Delta z < 0.01$.

By $z > 1$ the expectations are that dark energy is subdominant and hence measurements become degenerate with the information in the CMB. A measurement would test that expectation and potentially reveal a more exotic form of the dark energy [7]. Indeed, measurement of the geometric shifting of power spectrum rings at any redshift would complement luminosity distance ratios from supernovae with a purely geometric test and lend credence to any future detection of a dynamical dark energy component.

[1] D.N. Spergel *et al.*, astro-ph/0302209.
[2] W. Hu and N. Sugiyama, Astrophys. J. **471**, 542 (1996).
[3] D.J. Eisenstein and W. Hu, Astrophys. J. **496**, 605 (1998).
[4] A. Meiksen, M. White, and J.A. Peacock, Mon. Not. R. Astron. Soc. **304**, 851 (1999).
[5] D.J. Eisenstein, W. Hu, and M. Tegmark, Astrophys. J. Lett. **504**, L57 (1998).
[6] A. Cooray, W. Hu, D. Huterer, and M. Joffre, Astrophys. J. Lett. **557**, L7 (2001).
[7] D.J. Eisenstein, in Proceedings from Wide-Field Multi-Object Spectroscopy conference, ASP Conference Series astro-ph/0301623 (2003); H. Seo and D.J. Eisenstein, astro-ph/0307460.
[8] C. Alcock and B. Paczynski, Nature (London) **281**, 358 (1979).
[9] C. Blake and K. Glazebrook, astro-ph/0301632.

[10] E. Linder, astro-ph/0304001.
[11] T. Matsubara and A.S. Szalay, Astrophys. J. **574**, 1 (2002); Phys. Rev. Lett. **90**, 021302 (2003).
[12] H.A. Feldman, N. Kaiser, and J.A. Peacock, Astrophys. J. **426**, 23 (1994).
[13] J.E. Carlstrom, G.P. Holder, and E.D. Reese, Annu. Rev. Astron. Astrophys. **40**, 643 (2002).
[14] N. Kaiser, Mon. Not. R. Astron. Soc. **227**, 1 (1987).
[15] P. Coles, Mon. Not. R. Astron. Soc. **262**, 1065 (1993).
[16] M. Tegmark, A.J.S. Hamilton, M.A. Strauss, M.S. Vogeley, and A.S. Szalay, Astrophys. J. **499**, 555 (1998).
[17] A. Jenkins *et al.*, Mon. Not. R. Astron. Soc. **321**, 372 (2001).
[18] H.J. Mo and S.D.M. White, Mon. Not. R. Astron. Soc. **282**, 347 (1996).

[19] R.K. Sheth and B. Tormen, Mon. Not. R. Astron. Soc. **308**, 119 (1999).

[20] D.J. Eisenstein *et al.*, Astron. J. **122**, 2267 (2001).

[21] S. Majumdar and J.J. Mohr, Astrophys. J. **585**, 603 (2003).

[22] Z. Haiman and W. Hu (in preparation).

[23] S. Majumdar and J.J. Mohr, astro-ph/0305341.

[24] D.J. Eisenstein, W. Hu, and M. Tegmark, Astrophys. J. **518**, 2 (1999).

[25] W. Hu, Phys. Rev. D **65**, 023003 (2002).